

Multi-modal Multi-level Fusion for 3D Single Object Tracking

Zhiheng Li†, Yubo Cui†, Zuoxu Gu, and Zheng Fang*

Abstract—3D single object tracking plays a crucial role in computer vision. Mainstream methods mainly rely on point clouds to achieve geometry matching between target template and search area. However, textureless and incomplete point clouds make it difficult for single-modal trackers to distinguish objects with similar structures. To overcome the limitations of geometry matching, we propose a Multi-modal Multi-level Fusion Tracker (MMF-Track), which exploits the image texture and geometry characteristic of point clouds to track 3D target. Specifically, we first propose a Space Alignment Module (SAM) to align RGB images with point clouds in 3D space, which is the prerequisite for constructing inter-modal associations. Then, *in feature interaction level*, we design a Feature Interaction Module (FIM) based on dual-stream structure, which enhances intra-modal features in parallel and constructs inter-modal semantic associations. Meanwhile, in order to refine each modal feature, we introduce a Coarse-to-Fine Interaction Module (CFIM) to realize the hierarchical feature interaction at different scales. Finally, *in similarity fusion level*, we propose a Similarity Fusion Module (SFM) to aggregate geometry and texture clues from the target. Experiments show that our method achieves state-of-the-art performance on KITTI ($\sim 39\%$ Success and $\sim 42\%$ Precision gains against previous multi-modal method) and is also competitive on NuScenes.

I. INTRODUCTION

Recently, 3D single object tracking (SOT), as an important task of computer vision, has attracted much attention in autonomous driving. Most 3D SOT methods [1], [2], [3], [4], [5], [6], [7] inherit 2D Siamese paradigm [8], [9], [10] and estimate the current target state by geometry matching between the target template and search region, as shown in Fig. 1(a). However, due to these single-modal 3D trackers relying on sparse and textureless point clouds, it is difficult for them to identify target from the background with similar structures, such as tracking a specific person in the crowd. Fortunately, semantically rich images can provide fine-grained texture features that could help tracker to distinguish target from disturbances. Therefore, it is valuable to explore multi-modal 3D SOT and combine the advantage of image and point cloud.

F-Siamese [11] is the first multi-modal SOT tracker, which adopts cascaded structure to connect the 2D tracker with 3D tracker, as shown in Fig. 1(b). Specifically, F-Siamese first adopts 2D tracker to estimate 2D bounding box of target and projects it into 3D viewing frustum based on camera matrix. Then, the 3D tracker extracts frustum point features in the frustum and finally predicts the 3D target. However, F-Siamese ignores feature interaction between two modalities and loses

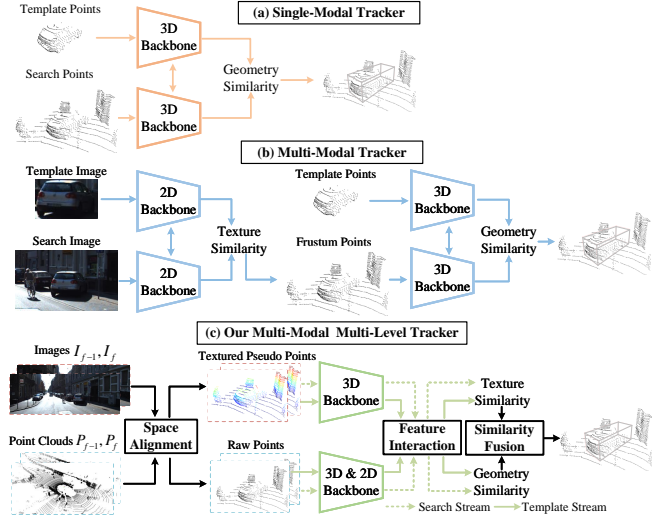


Fig. 1. Comparison of the current 3D single object tracking frameworks. (a) Single-modal paradigm adopts geometry matching of point clouds. (b) Multi-modal paradigm consists of 2D and 3D trackers in series. (c) Our MMF-Track employs dual-stream structure and includes three novel modules: space alignment, feature interaction and similarity fusion.

many important cues from target. Thus, its performance lags much behind LiDAR-Only methods.

Apart from the cascaded tracker, feature-level fusion is another effective way to aggregate multi-modal information, which has been verified in 3D object detection [12], [13], [14], [15], [16], [17]. For example, PointPainting [12] and PointAugmenting [13] utilize segmentation scores or semantic features of images to decorate point clouds in the early stage, while CLOCs [14] merges cross-modal features at the instance level. Besides, [15], [16], [17] deeply fuse hierarchical multi-modal features that are extracted from 2D and 3D backbones. However, due to the different frameworks and objectives between tracking and detection, 3D SOT has its own challenges: (1) **Data Alignment**. Since tracking usually requires two branches as input, multi-modal tracker should align different sensor data and search-template areas, which is more complex and challenging than 3D detection task. (2) **Feature Matching**. In order to locate the target within the search region, multi-modal tracker needs not only to focus on feature fusion but also consider effective feature matching between search and template branches.

To tackle the aforementioned issues, we propose a Multi-modal Multi-level Fusion Tracker (MMF-Track), which aims to guarantee data alignment for multi-sensor and integrate multi-modal information in the feature and similarity levels, as shown in Fig. 1(c). Due to heterogeneous representations between point cloud and image, it is non-trivial to effectively fuse 3D sparse points with 2D dense pixels. Thus, we

†Authors with equal contribution.

The authors are all with the Faculty of Robot Science and Engineering, Northeastern University, Shenyang, China; Corresponding author: Zheng Fang, e-mail: fangzheng@mail.neu.edu.cn

first propose a *Space Alignment Module* (SAM) to generate textured pseudo points aligned with raw points in 3D space. In this way, both of them can be further used to establish multi-modal semantic associations in the following network. Then, **in multi-modal feature interaction**, instead of simply combining two modal features, we propose a novel *Feature Interaction Module* (FIM) based on dual-stream network, learning intra-modal long-range contextual information in parallel and then establishing inter-modal semantic associations through attention mechanism. Meanwhile, due to limited semantic cues of single-scale feature, we further propose a *Coarse-to-Fine Interaction Module* (CFIM), which exploits multi-scale texture information to refine two modalities by interpolation and encoding operation. Moreover, **in geometry-texture similarity fusion**, different from previous methods that only utilize geometry similarity of raw points, we additionally generate texture similarity from pseudo points and adaptively fuse two similarities through *Similarity Fusion Module* (SFM). Thus, the texture and geometry cues of target are aggregated to search region, resulting in more robust tracking performance.

In summary, our contributions are as follows: **1)** We propose MMF-Track, a new multi-modal paradigm for 3D SOT, which leverages geometry and texture cues to track target. **2)** We propose SAM to align different modalities and introduce CFIM to facilitate layer-wise feature interaction via dual-stream structure. Additionally, we present SFM to aggregate the geometry and texture cues of target. **3)** MMF-Track achieves state-of-the-art tracking performance on KITTI and competitive results on NuScenes, outperforming the previous multi-modal method by a noticeable margin.

II. RELATED WORK

A. 2D Single Object Tracking

The success of deep learning in recent years has greatly encouraged researchers to propose many end-to-end 2D SOT methods [8], [9], [10], [18]. For example, SiamFC [8] is a milestone work in the 2D tracker. It proposed a novel Siamese structure and viewed tracking as a matching problem. That is, the current position and dimension of the target are estimated through matching search and template features. Soon after, SiamDW [9] explored how the width and depth of convolution neural networks affect tracker performance. Besides, SiamCAR [10] and SiamBAN [18] proposed a pixel-wise regression method to avoid generating numerous anchors. Moreover, many recent works [19], [20], [21], [22] have exploited Transformer [23] to achieve significant performance improvement. Although 2D trackers have obtained promising results in datasets and practical applications, they are difficult to handle 3D point clouds for 3D SOT.

B. 3D Single Object Tracking

Inspired by 2D SOT, the previous 3D SOT methods [2], [3], [6] usually compute point-wise similarity between the template and search branches. Specially, P2B [2] further embedded cosine similarity map with target clues into search feature and predicted the target through VoteNet [24]. Later,

BAT [3] proposed BoxCloud to encode the prior knowledge of target dimension to strengthen the similarity learning ability. Furthermore, V2B [6] voxelized discrete points to generate dense BEV features and regressed 3D target in a pixel-wise manner.

With the popularity of Transformer [23] in computer vision, some works [4], [5], [7], [25], [26] tried to apply Transformer to 3D SOT and obtained stronger tracking performance. Specifically, PTT [4] adopted attention mechanism to weigh point cloud features. LTTR [5] exploited Transformer to capture the inter- and intra- relations among different regions. Moreover, PTTR [7], STNet [25] and SMAT [26] proposed Transformer encoder-decoder to enhance and fuse features. Different from the above matching methods, M²-Track [27] proposed a motion-centric paradigm, which estimated the motion state through point clouds of consecutive frames. [27] had greatly overcome point cloud sparsity and achieved significant performance improvement. However, no matter the motion or matching paradigm, these methods relied on sparse point clouds, leading trackers to easily confuse geometrically similar objects. To the best of our knowledge, there are few works exploring the multi-modal 3D SOT task. F-Siamese [11] is the most recently multi-modal tracker, which utilized 2D tracking result to generate 3D frustum and adopted 3D tracker to predict target. However, its cascaded structure limits potential capabilities of multi-modal tracker.

C. Multi-modal Feature Fusion in 3D Object Detection

To overcome the inherent defects in each sensor, many 3D detection methods combine the advantage of image and point cloud through feature fusion. And these methods can be divided into three categories: *early fusion* [12], [13], *late fusion* [14] and *deep fusion* [15], [16], [17]. For example, PointPainting [12] appended image segmentation scores to each point and generated painted points as network input. Different from [12], CLOCs [14] generated 2D and 3D proposals, which were merged at the object level. Besides, most works (e.g. EPNet [15]) deeply fused features extracted from different backbones and made full use of semantic information in multi-modal. Inspired by the above works, we design a feature interaction network that is more suitable for tracking task and propose a novel similarity fusion method to aggregate texture and geometry clues of target.

III. METHODOLOGY

A. Overview

Given an initial bounding box $B_0 = (x_0, y_0, z_0, w, h, l, \theta_0) \in R^7$ of the specific target at the first frame, 3D single object tracking aims to use sensor data to predict the target state $B_f = (x_f, y_f, z_f, \theta_f) \in R^4, f \in \{1, \dots, m\}$ frame by frame, where (x, y, z) is the bounding box center, and θ is the heading angle. Following the previous works, we assume that the target size (w, h, l) is unchanged during tracking.

According to the number of modalities employed, trackers can be divided into single-modal and multi-modal. And the former can be formulated as follows:

$$\Psi(B_{f-1}, P_{f-1}, P_f) \mapsto B_f \quad (1)$$

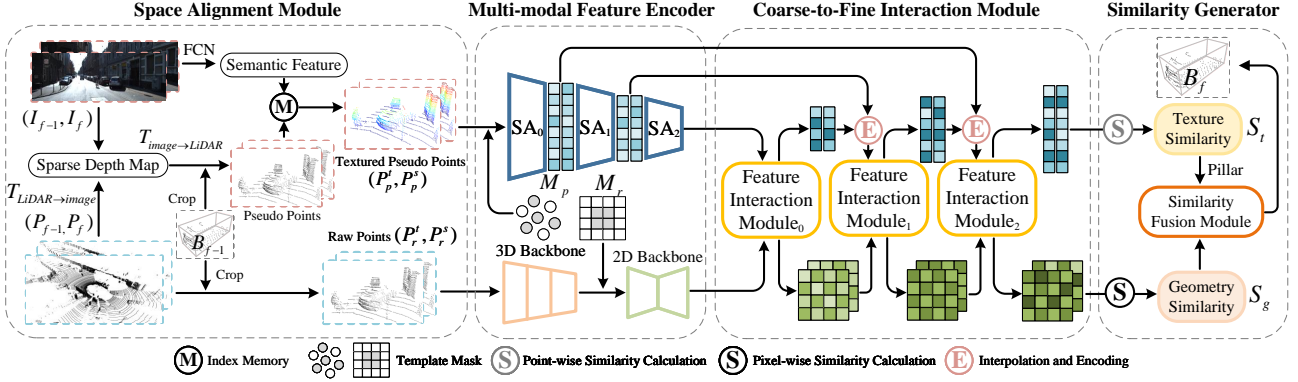


Fig. 2. **Overview of our proposed MMF-Track.** The network consists of four steps: (a) *Space Alignment Module* generates textured pseudo points parallel to the raw points branch. (b) *Multi-modal Feature Encoder* extracts discriminative features from two modalities. (c) *Coarse-to-Fine Interaction Module* adopts *Feature Interaction Module* and interpolation operation to enhance intra-modal features and construct inter-modal associations iteratively. (d) *Similarity Generator* generates geometry and texture similarities and then fuses them via *Similarity Fusion Module* for regressing the target.

where P_{f-1}, P_f are two consecutive point clouds. Furthermore, multi-modal tracker [11] adds image tracking phase before 3D tracker, forming a two-stage tracking paradigm:

$$\Pi(\hat{B}_{f-1}, I_{f-1}, I_f) \mapsto \hat{B}_f \quad (2)$$

$$\Phi(B_{f-1}, \hat{B}_f, P_{f-1}, P_f) \mapsto B_f \quad (3)$$

where $(I_{f-1}, I_f), (\hat{B}_{f-1}, \hat{B}_f)$ represent images and predicted 2D bounding boxes in the last and current frames respectively. Different from above paradigms, we design a dual-stream network that processes multi-modal features in parallel, which is shown in Fig. 2 and formulated as follows:

$$\Gamma(B_{f-1}, I_{f-1}, I_f, P_{f-1}, P_f) \mapsto B_f \quad (4)$$

B. Data Alignment and Feature Extraction

1) *Space Alignment Module*: Due to heterogeneous representations between images and point clouds, we propose a Space Alignment Module (SAM) to ensure multi-modal spatial alignment. Specifically, we first project point clouds $P \in \{P_{f-1}, P_f\}$ to the image plane through projection matrix $T_{LiDAR \rightarrow image}$ and allocate the depth of each point to its nearest pixel I_{ij} . Thus, we can generate a sparse depth map $S \in R^{W \times H \times 1}$ and then convert S into pseudo points by matrix $T_{image \rightarrow LiDAR}$. When given B_{f-1} in the last frame, we crop out multi-modal search-template points and store indexes that indicate the projection relationship between pixels and pseudo points. Inspired by [13], we further adopt FCN [28] to extract semantic feature $H \in R^{W \times H \times D}$ and append H to pseudo points by index memory. Finally, SAM output textured pseudo points (P'_p, P''_p) and raw points (P'_r, P''_r) .

Our SAM has the following novelties: 1) Different from [13] using image features to augment raw points, we generate textured pseudo points parallel to raw points branch, which is convenient for subsequent multi-modal semantic association. Besides, FCN can be trained with our network and online decorate points rather than offline painting features in [13]. 2) Instead of viewing the points in B_{f-1} as template, we argue that contextual information of background can help tracker perceive target motion. Thus, we crop out the template with the same size as search region and use template mask M to distinguish the target from backgrounds.

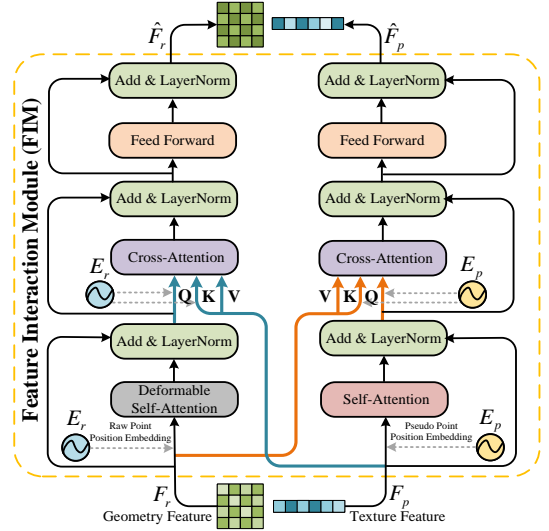


Fig. 3. **Dual-stream structure of Feature Interaction Module (FIM).** Self-attention and cross-attention are utilized to enhance two modal features and construct semantic associations.

2) *Multi-modal Feature Encoder*: For the pseudo points, the mask M_{p_i} ($i \in \{1, 2, \dots, N\}$) indicates whether the template point P'_{p_i} is located in B_{f-1} by padding with 1 or 0, where N is the number of points. After combining points P'_p with mask $M_p \in R^{N \times 1}$, we feed $P_p \in \{P'_p \odot M_p, P''_p\}$ into PointNet++ [29] to generate texture feature $F_p = \{F'_p, F''_p\} \in R^{N \times D}$:

$$F'_p = \text{PointNet++}_1(P'_p \odot M_p), F''_p = \text{PointNet++}_2(P''_p) \quad (5)$$

where \odot means feature concatenation along channel dimension. For the raw points, we first use 3D backbone of SECOND [30] to generate dense BEV features $G_r = \{G'_r, G''_r\} \in R^{W_1 \times H_1 \times D}$ and merge G'_r with M_r . Note that $M_r \in R^{W_1 \times H_1 \times 1}$ is similar to M_p but projected to BEV plane. Then, we adopt a group of convolution as 2D Backbone to further encode G_r and get geometry feature $F_r = \{F'_r, F''_r\} \in R^{W_1 \times H_1 \times D}$:

$$F'_r = \text{Conv}_1(G'_r \odot M_r), F''_r = \text{Conv}_2(G''_r) \quad (6)$$

C. Feature Enhancement and Interaction

In this part, we design a dual-stream structure to propagate multi-modal information bidirectionally and propose

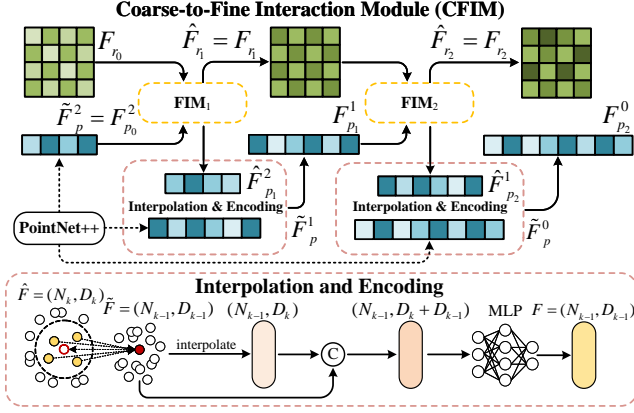


Fig. 4. **Detail of Coarse-to-Fine Interaction Module (CFIM).** CFIM uses multi-scale information to refine multi-modal features iteratively by Interpolation and Encoding operation as well as Feature Interaction Module.

a coarse-to-fine strategy to refine each modal iteratively. To simplify description, we explain the search branch that is the same as the template and replace (F_p^s, F_r^s) with (F_p, F_r) .

1) *Feature Interaction Module*: To enhance multi-modal features that represent the same semantic object, we propose a Feature Interaction Module (FIM) composed of intra-modal feature enhancement and inter-modal semantic interaction.

Intra-modal Feature Enhancement. In Fig. 3, we adopt vanilla self-attention to learn long-range contextual information in F_p and obtain a more discriminative texture feature \mathcal{F}_p by attention weights. Meanwhile, to reduce computational complexity of attention mechanism, we employ deformable attention [31] to F_r and get a non-local geometry feature \mathcal{F}_r . The process of feature enhancement is described as follows:

$$Q = \alpha(F) + E, K = \beta(F) + E, V = \gamma(F) \quad (7)$$

$$\mathcal{F}_p = \text{LN}(\text{SelfAttn}(Q_p, K_p, V_p)) + Q_p \quad (8)$$

$$\mathcal{F}_r = \text{LN}(\text{DeformAttn}(Q_r, K_r, V_r)) + Q_r \quad (9)$$

where $E \in \{E_p, E_r\}$ is the position encoding of two modalities. LN means layer normalization, and α, β, γ represent three linear layers with non-shared weights.

Inter-modal Feature Interaction. Due to the two modalities focusing on different information, we design a dual-stream structure to realize bilateral interaction rather than the classical unilateral fusion. To construct semantic association between the texture and geometry features, we first convert \mathcal{F}_r to Q_r by Eq. 7 in the geometry branch and map F_p to $(\mathcal{K}_p, \mathcal{V}_p)$ in another branch. Then, we feed $(Q_r, \mathcal{K}_p, \mathcal{V}_p)$ to cross-attention operation, which encodes semantic consistent texture information to geometry feature and generate a more robust feature representation \mathcal{F}_r . Meanwhile, in the texture branch, we also utilize the same approach to enhance the semantic information of texture feature \mathcal{F}_p :

$$\mathcal{F}_p = \text{LN}(\text{CrossAttn}(Q_p, \mathcal{K}_r, \mathcal{V}_r)) + Q_p \quad (10)$$

$$\mathcal{F}_r = \text{LN}(\text{CrossAttn}(Q_r, \mathcal{K}_p, \mathcal{V}_p)) + Q_r \quad (11)$$

Finally, we feed $(\mathcal{F}_p, \mathcal{F}_r)$ to fully connected feed-forward network and generate enhanced features (\hat{F}_p, \hat{F}_r) . After the above steps, we not only realize multi-modal interaction

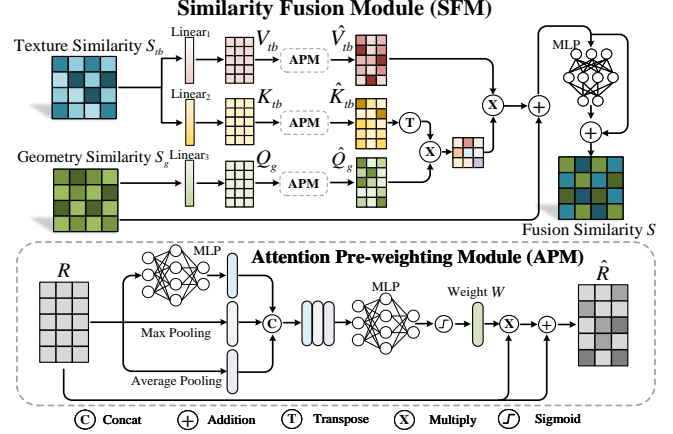


Fig. 5. **Structure of Similarity Fusion Module (SFM).** SFM enhances each-modal similarity through Attention Pre-weighting Module (APM) before adaptively fusing geometry and texture similarities.

but also retain each modal feature independently. Thus the features can be refined iteratively and generate geometry and texture similarities in the following modules.

2) *Coarse-to-Fine Interaction Module*: Although simply stacking FIM can enhance two modal features, it is still difficult to construct complex semantic associations depending on single-scale features. Meanwhile, due to down-sampling operation in the feature encoder, the number of texture features becomes very small at the end, limiting multi-modal interaction in FIM. Therefore, we propose Coarse-to-Fine Interaction Module (CFIM) that exploits multi-scale features to achieve multi-modal interaction layer by layer and finally obtains finer features. As shown in Fig. 4, we first utilize layer-wise texture features $\hat{F}_p^k \in \mathbb{R}^{N_k \times D_k}$ ($k \in \{0, 1, 2\}$) extracted by PointNet++ [29] as the source of multi-scale information, where N_k, D_k mean the seed point number and channel dimension in the k -th set-abstraction layer. Then, in the j -th CFIM layer ($j \in \{1, 2\}$), we adopt FIM _{j} to interact $F_{p_{j-1}}^k$ with $F_{r_{j-1}}$ and generate $\hat{F}_{p_j}^k \in \mathbb{R}^{N_k \times D_k}, \hat{F}_{r_j} \in \mathbb{R}^{W_1 \times H_1 \times D_k}$.

$$\hat{F}_{p_j}^k, \hat{F}_{r_j} = \text{FIM}_j(F_{p_{j-1}}^k, F_{r_{j-1}}) \quad (12)$$

Later, following feature propagation in [29], we interpolate $\hat{F}_{p_j}^k$ with \hat{F}_p^{k-1} and use a MLP to generate feature $F_{p_j}^{k-1} \in \mathbb{R}^{N_{k-1} \times D_{k-1}}$ by Eq. 13, where τ is the interpolation function.

$$F_{p_j}^{k-1} = \text{MLP}(\text{Concat}(\tau(\hat{F}_{p_j}^k, \hat{F}_p^{k-1}), \hat{F}_p^{k-1})) \quad (13)$$

Finally, by repeating the above processes, our CFIM can utilize multi-scale information to complement and refine multi-modal features iteratively.

D. Similarity Generation and Fusion

Similarity Generation. For geometry features (F_r^t, F_r^s) from CFIM, we calculate pixel-wise similarity [33] and generate geometry similarity $S_g \in \mathbb{R}^{H_1 \times W_1 \times D}$. Meanwhile, for texture feature (F_p^t, F_p^s) , we first adopt cosine distance as metric and generate point-wise texture similarity $S_t \in \mathbb{R}^{N_0 \times D}$. Then, to ensure feature alignment, we perform pillarization process by Max Pooling to convert S_t into BEV feature $S_{tb} \in \mathbb{R}^{H_1 \times W_1 \times D}$.

TABLE I

PERFORMANCE COMPARISON ON THE KITTI DATASET. L MEANS LiDAR-ONLY METHODS, WHILE L+C REPRESENTS LiDAR-CAMERA METHODS.

Method	Modality	Car-6424		Pedestrian-6088		Van-1248		Cyclist-308		Mean-14068/12820	
		Success	Precision	Success	Precision	Success	Precision	Success	Precision	Success	Precision
SC3D [1]	L	41.3	57.9	18.2	37.8	40.4	47.0	41.5	70.4	31.2	48.5
BAT [3]		60.5	77.7	42.1	70.1	52.4	67.0	33.7	45.4	51.2	72.8
PTT [4]		67.8	81.8	44.9	72.0	43.6	52.5	37.2	47.3	55.1	74.2
LTTR [5]		65.0	77.1	33.2	56.8	35.8	45.6	66.2	89.9	48.7	65.8
V2B [6]		70.5	81.3	48.3	73.5	50.1	58.0	40.8	49.7	58.4	75.2
PTTR [7]		65.2	77.4	50.9	81.6	52.5	61.8	65.1	90.5	57.9	78.1
SMAT [26]		71.9	82.4	52.1	81.5	41.4	53.2	61.2	87.3	60.4	79.5
STNet [25]		72.1	84.0	49.9	77.2	58.0	70.6	73.5	93.7	61.3	80.1
M ² -Track [27]		65.5	80.8	61.5	88.2	53.8	70.7	73.2	93.5	62.9	83.4
F-Siamese [11]		L+C	37.1	50.6	16.3	32.3	-	-	47.0	77.3	27.5
MMF-Track (Ours)	L+C	73.9	84.1	61.7	89.3	59.3	72.5	75.9	95.0	67.4	85.6
<i>Improvement</i>		↑36.8	↑33.5	↑45.4	↑57.0	-	-	↑28.9	↑17.7	↑39.9	↑42.7

TABLE II

PERFORMANCE COMPARISON ON THE NUSCENES DATASET. * REPRESENTS THE RESULTS WE TESTED WITH THE OFFICIAL CODE.

Method	Modality	Car-64159		Pedestrian-33227		Truck-13587		Bicycle-2292		Mean-113265	
		Success	Precision	Success	Precision	Success	Precision	Success	Precision	Success	Precision
SC3D [1]	L	22.31	21.93	11.29	12.65	30.67	27.73	16.70	28.12	19.97	19.88
P2B [2]		38.81	43.18	28.39	52.24	42.95	41.59	26.32	47.80	36.00	45.72
BAT [3]		40.73	43.29	28.83	53.32	45.34	42.58	27.17	51.37	37.52	46.31
PTT [4]		41.22	45.26	19.33	32.03	50.23	48.56	28.39	51.19	35.62	41.89
SMAT [26]		43.51	49.04	32.27	60.28	44.78	44.69	25.74	61.06	40.01	52.06
M ² -Track [27]		55.85	65.09	<u>32.10</u>	<u>60.92</u>	57.36	59.54	36.32	<u>67.50</u>	48.67	63.25
TransFusion* [32]		L+C	37.42	46.52	12.85	26.82	28.86	33.57	19.45	41.96	28.94
MMF-Track (Ours)	L+C	<u>50.73</u>	<u>58.51</u>	30.75	65.16	<u>54.18</u>	<u>57.73</u>	<u>30.90</u>	69.24	<u>44.88</u>	<u>60.58</u>

Similarity Fusion. We propose a Similarity Fusion Module (SFM) that adaptively fuses S_g with S_{tb} and aggregates geometry and texture clues from target. Specifically, as shown in Fig. 5, we first use three linear layers to generate attention vector Q_g, K_{tb}, V_{tb} , respectively. Then, to maximize the use of significant information in each-modal similarity, we propose an Attention Pre-weighting Module (APM) to enhance target clues in attention vector. The APM is described as follows:

$$W = \sigma(\text{MLP}(\text{Concat}(\text{MLP}(R), \text{Max}(R), \text{Avg}(R)))) \quad (14)$$

$$\hat{R} = RW + R \quad (15)$$

where σ is the sigmoid function and $R \in \{Q_g, K_{tb}, V_{tb}\}$, $\hat{R} \in \{\hat{Q}_g, \hat{K}_{tb}, \hat{V}_{tb}\}$. Max and Avg represent Max Pooling and Average Pooling, respectively. Finally, we use the pre-weighted attention vector $\hat{Q}_g, \hat{K}_{tb}, \hat{V}_{tb}$ to calculate the attention weight and achieve similarity fusion by Eq. 16.

$$\hat{S} = \frac{\hat{Q}_g \hat{K}_{tb}^T}{\sqrt{d_k}} \hat{V}_{tb} + S_g, S = \text{MLP}(\hat{S}) + \hat{S} \quad (16)$$

where $\sqrt{d_k}$ is the scale factor. Different from vanilla cross-attention, our proposed SFM adaptively enhances the critical target clues in geometry and texture similarities before exchanging information with each other. Thus, compared with simply stacking, adding, or directly using cross-attention, SFM can obtain a more discriminative similarity feature S .

E. Prediction and Training

Following CenterPoint [34], we use fusion similarity S to predict the target’s spatial location and orientation in a center manner. The training loss is formulated as follows:

$$L = \lambda_{cls} L_{cls} + \lambda_{reg} L_{reg} \quad (17)$$

where we use focal loss [35] as L_{cls} to train heatmap classification and adopt L1 loss as L_{reg} for box regression. λ_{cls} and λ_{reg} are weights for the two losses, respectively.

IV. EXPERIMENTS

A. Experimental Settings

Datasets. We train and evaluate our method on KITTI [36] and NuScenes [37] datasets. And we follow [2], [3] to split KITTI as follows: scenes 0-16 for training, scenes 17-18 for validation, and scenes 19-20 for testing. For NuScenes, the training and validation sets are consistent with [27].

Evaluation Metrics. Following the evaluation metrics of [2], [3], we utilize *Success* and *Precision* defined in the one pass evaluation (OPE) to evaluate tracking performance.

Implementation Details. In data processing, we set the point cloud range as $[-3.2m, 3.2m]$ for the X and Y axes, and $[-3m, 1m]$ for the Z axis. Following [5], we set voxel size as $[0.025m, 0.025m, 0.05m]$ and voxelize template-search points in raw point branch. And we process the number of points to $N = 1024$ by randomly copying and discarding in pseudo point branch. Then, we adopt PointNet++ [29] consisting of three set-abstraction (SA) layers to encode pseudo points. The ball-query radii are set to $0.3m$, $0.5m$ and $0.7m$. We train 40 epochs for MMF-Track with Adam optimizer and set batch size 32 on NVIDIA 2080Ti GPU.

B. State-of-the-arts Comparison

Quantitative results on KITTI. In Tab. I, we compare our MMF-Track with previous LiDAR-Only and LiDAR-Camera

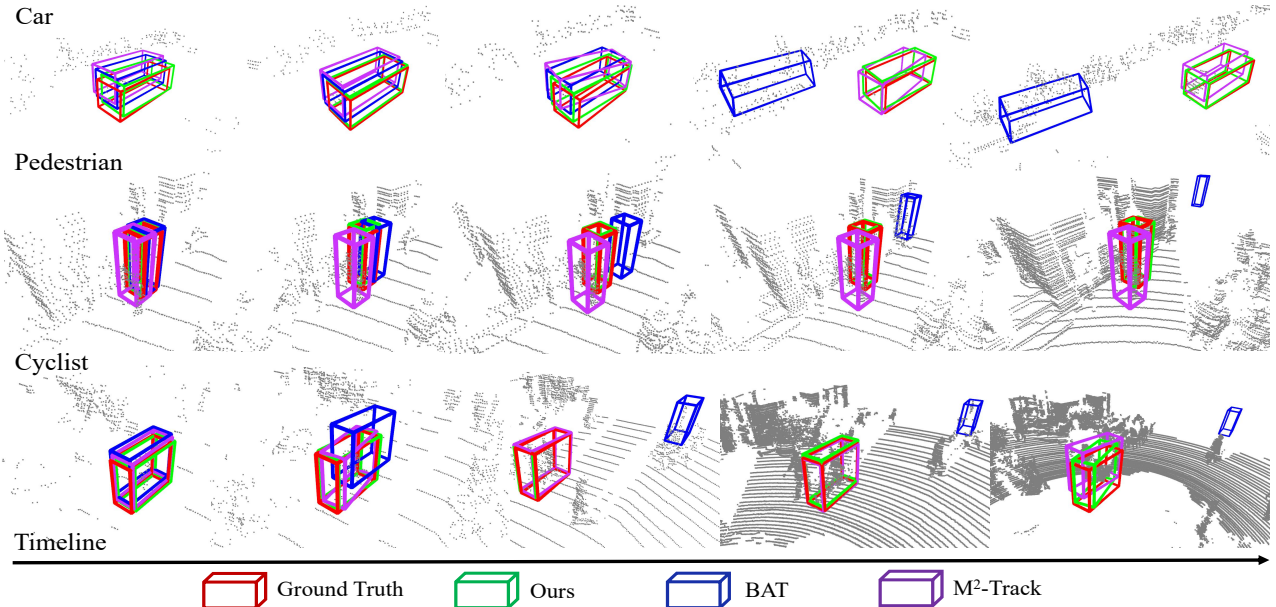


Fig. 6. Visualization tracking results on KITTI dataset. From top to bottom, we compare our MMF-Track with BAT, M²-Track and show the cases of Car, Pedestrian and Cyclist categories.

methods. The results demonstrate that our method achieves the best performance in all evaluation metrics and categories. Compared with previous state-of-the-art LiDAR-Only method M²-Track [27], our method outperforms it by 4.5% and 2.2% on *Mean Success* and *Precision*, verifying that our multi-modal method has certain advantages over single-modal. Moreover, compared with LiDAR-Camera method F-Siamese [11], we achieve significant performance improvement (39.9%/42.7% on *Mean Success/Precision*). This proves that by multi-modal interaction and geometry-texture similarity fusion, we can effectively integrate target clues from different modalities and achieve better performance.

Quantitative results on NuScenes. Since there is no multi-modal SOT method evaluated on NuScenes, we additionally employ the SOTA multi-modal detection method, TransFusion [32], to perform multi-object tracking and then transfer its results into the SOT task. As shown in Tab. II, our method outperforms [32] because it is difficult for TransFusion to use target-specific features to track a single object. Besides, our method obtains the best results among similarity-based methods [1], [2], [3], [4], [26], proving that our method can improve tracking performance by effectively combining geometry and texture similarities. Then, compared with the motion-based method [27], our method has advantages in tracking small-size objects. Specially for Pedestrians with small point numbers, our method achieves 65.16% in *Precision* and outperforms [27] by 4.24%.

Visualization results on KITTI. We visualize tracking results of different categories in Fig. 6. In the scene with a few points, such as the 1st row, BAT is easily interfered with by backgrounds, resulting in target loss. But our method can overcome the impact of point cloud sparsity and better distinguish the target and backgrounds. When there are some objects similar to target (in the 2nd row), the M²-Track and BAT both incorrectly track similar objects due to depending

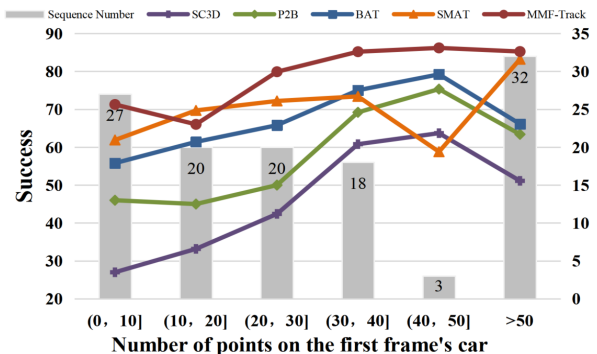


Fig. 7. Effect of the number of points in the first frame. In most cases, our MMF-Track outperforms other methods with remarkable margins.

on textureless points. By contrast, our method achieves robust tracking by exploiting texture features. Our method also obtains better tracking results for Cyclist in the 3rd row. **Robustness to Sparsity.** In Fig. 7, following [1], [2], [3], [26], we show tracking performance under the different number of points in the first frame. We can observe that our method maintains high performance in most cases and has better robustness than other single-modal methods.

Running speed. MMF-Track achieves 13 FPS on a single NVIDIA 2080Ti GPU and makes certain progress compared with the 5 FPS of multi-modal F-Siamese [11].

C. Ablation Study

We conduct ablation studies to validate our method. Most experiments are performed on the Car category of KITTI. **Model Components.** In Tab. III, we demonstrate the effectiveness of our modules. Due to A1 only relying on geometry matching of point clouds, its tracking result is not ideal. Then, compared with A5, removing any modules (in A2~A4) will result in performance degradation. Thus, every module is indispensable for the network. Specifically, A2 reflects that the template mask plays a critical role and

TABLE III

ABLATION STUDIES ON MODEL COMPONENTS. CFIM MEANS COARSE-TO-FINE INTERACTION MODULE. SFM REPRESENTS SIMILARITY FUSION MODULE. TM IS THE TEMPLATE MASK.

	Modality	TM	CFIM	SFM	3D Success	3D Precision
A1	L	✗	✗	✗	65.4 \downarrow 8.5	74.6 \downarrow 9.5
A2	L+C	✗	✓	✓	70.4 \downarrow 3.5	80.7 \downarrow 3.4
A3	L+C	✓	✗	✓	70.6 \downarrow 3.3	81.0 \downarrow 3.1
A4	L+C	✓	✓	✗	70.0 \downarrow 3.9	79.5 \downarrow 4.6
A5	L+C	✓	✓	✓	73.9	84.1

TABLE IV

ABLATION OF THE STREAM STRUCTURE AND FEATURE INTERACTION METHODS. FIM IS THE FEATURE INTERACTION MODULE.

	Stream Structure	Interaction Strategy	3D Success	3D Precision
B1	Two-in-One	Single Cross-Attention	68.4	78.8
B2	Dual-Stream	Single FIM	70.2	80.8
B3	Dual-Stream	Stacking n FIMs	71.9	82.1
B4	Dual-Stream	CFIM	73.9	84.1

TABLE V

ABLATION STUDIES OF SIMILARITY FUSION STRATEGIES.

	Similarity Fusion Strategy	3D Success	3D Precision
C1	Addition	71.4	80.7
C2	Concat	71.3	81.8
C3	Cross-Attention	70.6	80.3
C4	SFM	73.9	84.1

TABLE VI

ABLATION STUDIES OF DIFFERENT PAINTING STRATEGIES.

	Painting Strategy	3D Success	3D Precision
D1	w/o Painting	67.9	77.1
D2	w/ RGB	71.5	81.2
D3	w/ Feature Offline	72.0	82.3
D4	w/ Feature Online	73.9	84.1

helps tracker perceive target well by contextual background. Besides, as shown in A3 and A4, lacking multi-modal interaction or similarity fusion will also cause bad results, especially in A4, which proves that effectively using multi-modal information is the key to multi-modal tracker.

Feature Interaction. We compare different feature interaction methods in Tab. IV. First, as shown in B1, although cross-attention is commonly used to fuse different modalities, it is not enough to construct complex multi-modal associations. Instead of simple two-in-one manner, FIM can enhance intra-modal features and construct inter-modal associations, which improves *Success/Precision* by 1.8%/2.0%. Then, we can obtain further performance improvement by stacking $n = 3$ FIMs. Lastly, benefiting from the coarse-to-fine strategy, B4 achieves the best performance, higher than B3 with 2.0% in both *Success* and *Precision*, which proves that our CFIM has a stronger ability to construct semantic association.

Similarity Fusion. As shown in Tab. V, we compare different similarity fusion strategies. Our proposed SFM achieves the best performance in C4, surpassing C1 by 2.5% and 3.4% in *Success* and *Precision*, respectively. Then, compared with directly using cross-attention in C3, our method obtains 3.3% and 3.8% improvement, showing the effectiveness of APM. It is interesting that the performance of C3 is lower

TABLE VII

THE RESULTS OF DIFFERENT TEMPLATE GENERATION STRATEGIES.

Strategy	PTT [4]	V2B [6]	SMAT [26]	MMF-Track
First GT	62.9/76.5	67.8/79.3	68.1/77.5	69.2/79.8
Previous result	64.9/77.5	70.0/81.3	66.7/76.1	71.9/81.9
First GT & Previous result	67.8/81.8	70.5/81.3	71.9/82.4	73.9/84.1
All previous results	59.8/74.5	69.8/81.2	69.9/79.8	71.7/81.4

TABLE VIII

COMPARISON TRACKING PERFORMANCE W/ OR W/O IMAGE BRANCH ON THE NUSCENES.

Image Branch	Car	Pedestrian	Truck	Bicycle	Mean
✓	50.73/58.51	30.75/65.16	54.18/57.73	30.90/69.24	44.88/60.58
✗	33.95/44.69	25.22/60.03	49.16/52.44	25.50/62.15	33.04/50.47
Decreasing	16.78/13.82	5.53/5.13	5.02/5.29	5.40/7.09	11.84/10.11

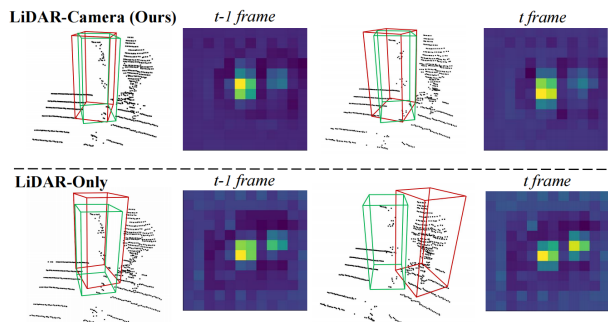


Fig. 8. Visual comparison of tracking results and heatmaps from two consecutive frames. The predicted and ground-truth boxes are in red and green, respectively.

than C1 and C2. We think that it's because directly using cross-attention may break the similarity between template and search features. But thanks to our APM that adaptively adjusts each-modal similarity in advance, we can effectively aggregate geometry-texture clues in the subsequent step.

Painting Strategy. In Tab. VI, we compare different painting strategies for pseudo points. Instead of not painting any information in D1, appending RGB to pseudo points achieves better results in D2 (3.6%/4.1% improvement). Furthermore, following [13], we use semantic features extracted from an offline network to paint pseudo points in D3 and outperform D2 by 0.5%/1.1%. But the offline network can not be trained with tracker and will limit tracking performance. In contrast, in D4, our SAM can realize online painting and end-to-end training for the whole network, resulting in the best results.

Template Generation Strategy. We compare MMF-Track with previous works under the different template generation strategies. In Tab. VII, our method achieves the best and relatively stable results on four template generation schemes, which proves the superiority of our multi-modal method.

LiDAR-Camera vs. LiDAR-Only. To further verify the role of image in tracking, we first validate MMF-Track without image branch on NuScenes. As shown in Tab. VIII, the tracker occurs obvious performance degradation without texture feature. Then, for Pedestrian, we visualize tracking results of two consecutive frames and the corresponding heatmap in Fig. 8. The results show that the texture features extracted from the image can help tracker distinguish target

correctly when the point cloud is extremely sparse. Thus, we believe that image plays an important role in tracking.

V. CONCLUSION

In this paper, we propose a new multi-modal paradigm MMF-Track for 3D SOT task. First, we design Space Alignment Module to generate textured pseudo points aligned with the raw points in 3D Space. Then, we propose a novel dual-stream structure to enhance intra-modal features and construct inter-modal semantic associations. Finally, we present a Similarity Fusion Module to aggregate geometry and texture clues from the target. Experiments show that MMF-Track significantly outperforms previous multi-modal methods and achieves competitive results. We hope our work will inspire researchers to further study multi-modal tracking.

REFERENCES

- [1] S. Giancola, J. Zarzar, and B. Ghanem, "Leveraging shape completion for 3d siamese tracking," in *Proceedings of the IEEE/CVF Conference on Computer Vision and Pattern Recognition*, 2019.
- [2] H. Qi, C. Feng, Z. Cao, F. Zhao, and Y. Xiao, "P2b: Point-to-box network for 3d object tracking in point clouds," in *IEEE/CVF Conference on Computer Vision and Pattern Recognition*, 2020.
- [3] C. Zheng, X. Yan, J. Gao, W. Zhao, W. Zhang, Z. Li, and S. Cui, "Box-aware feature enhancement for single object tracking on point clouds," 2021.
- [4] J. Shan, S. Zhou, Z. Fang, and Y. Cui, "Ptt: Point-track-transformer module for 3d single object tracking in point clouds," 2021.
- [5] Y. Cui, Z. Fang, J. Shan, Z. Gu, and S. Zhou, "3d object tracking with transformer," 2021.
- [6] L. Hui, L. Wang, M. Cheng, J. Xie, and J. Yang, "3d siamese voxel-to-bev tracker for sparse point clouds," 2021.
- [7] C. Zhou, Z. Luo, Y. Luo, T. Liu, L. Pan, Z. Cai, H. Zhao, and S. Lu, "Pptr: Relational 3d point cloud object tracking with transformer," in *CVPR*, pp. 8531–8540, 2022.
- [8] L. Bertinetto, J. Valmadre, J. F. Henriques, A. Vedaldi, and P. H. S. Torr, "Fully-convolutional siamese networks for object tracking," in *European Conference on Computer Vision Workshops* (G. Hua and H. Jégou, eds.), pp. 850–865, 2016.
- [9] Z. Zhang and H. Peng, "Deeper and wider siamese networks for real-time visual tracking," in *Proceedings of the IEEE/CVF Conference on Computer Vision and Pattern Recognition*, pp. 4591–4600, 2019.
- [10] D. Guo, J. Wang, Y. Cui, Z. Wang, and S. Chen, "Siamcar: Siamese fully convolutional classification and regression for visual tracking," in *Proceedings of the IEEE/CVF conference on computer vision and pattern recognition*, pp. 6269–6277, 2020.
- [11] H. Zou, J. Cui, X. Kong, C. Zhang, Y. Liu, F. Wen, and W. Li, "F-siamese tracker: A frustum-based double siamese network for 3d single object tracking," in *IEEE/RSJ International Conference on Intelligent Robots and Systems*, pp. 8133–8139, 2020.
- [12] S. Vora, A. H. Lang, B. Helou, and O. Beijbom, "Pointpainting: Sequential fusion for 3d object detection," in *Proceedings of the IEEE/CVF conference on computer vision and pattern recognition*, pp. 4604–4612, 2020.
- [13] C. Wang, C. Ma, M. Zhu, and X. Yang, "Pointaugmenting: Cross-modal augmentation for 3d object detection," in *Proceedings of the IEEE/CVF Conference on Computer Vision and Pattern Recognition*, pp. 11794–11803, 2021.
- [14] S. Pang, D. Morris, and H. Radha, "Clocs: Camera-lidar object candidates fusion for 3d object detection," in *IEEE/RSJ International Conference on Intelligent Robots and Systems*, pp. 10386–10393, 2020.
- [15] T. Huang, Z. Liu, X. Chen, and X. Bai, "Epnet: Enhancing point features with image semantics for 3d object detection," in *European Conference on Computer Vision*, pp. 35–52, 2020.
- [16] Y. Li, A. W. Yu, T. Meng, B. Caine, J. Ngiam, D. Peng, J. Shen, Y. Lu, D. Zhou, Q. V. Le, et al., "Deepfusion: Lidar-camera deep fusion for multi-modal 3d object detection," in *Proceedings of the IEEE/CVF Conference on Computer Vision and Pattern Recognition*, pp. 17182–17191, 2022.
- [17] Z. Chen, Z. Li, S. Zhang, L. Fang, Q. Jiang, F. Zhao, B. Zhou, and H. Zhao, "Autoalign: Pixel-instance feature aggregation for multi-modal 3d object detection," *arXiv preprint arXiv:2201.06493*, 2022.
- [18] Z. Chen, B. Zhong, G. Li, S. Zhang, and R. Ji, "Siamese box adaptive network for visual tracking," in *Proceedings of the IEEE/CVF conference on computer vision and pattern recognition*, pp. 6668–6677, 2020.
- [19] S. Gao, C. Zhou, C. Ma, X. Wang, and J. Yuan, "Aiatrack: Attention in attention for transformer visual tracking," in *European Conference on Computer Vision*, pp. 146–164, Springer, 2022.
- [20] N. Wang, W. Zhou, J. Wang, and H. Li, "Transformer meets tracker: Exploiting temporal context for robust visual tracking," in *Proceedings of the IEEE/CVF Conference on Computer Vision and Pattern Recognition*, pp. 1571–1580, 2021.
- [21] X. Chen, B. Yan, J. Zhu, D. Wang, X. Yang, and H. Lu, "Transformer tracking," in *Proceedings of the IEEE/CVF Conference on Computer Vision and Pattern Recognition*, pp. 8126–8135, 2021.
- [22] Z. Fu, Q. Liu, Z. Fu, and Y. Wang, "Stmtrack: Template-free visual tracking with space-time memory networks," in *Proceedings of the IEEE/CVF Conference on Computer Vision and Pattern Recognition*, pp. 13774–13783, 2021.
- [23] A. Vaswani, N. Shazeer, N. Parmar, J. Uszkoreit, L. Jones, A. N. Gomez, L. u. Kaiser, and I. Polosukhin, "Attention is all you need," in *Advances in Neural Information Processing Systems*, vol. 30, Curran Associates, Inc., 2017.
- [24] C. R. Qi, O. Litany, K. He, and L. J. Guibas, "Deep hough voting for 3d object detection in point clouds," in *Proceedings of the IEEE/CVF International Conference on Computer Vision*, 2019.
- [25] L. Hui, L. Wang, L. Tang, K. Lan, J. Xie, and J. Yang, "3d siamese transformer network for single object tracking on point clouds," *arXiv preprint arXiv:2207.11995*, 2022.
- [26] Y. Cui, J. Shan, Z. Gu, Z. Li, and Z. Fang, "Exploiting more information in sparse point cloud for 3d single object tracking," *IEEE Robotics and Automation Letters*, vol. 7, no. 4, pp. 11926–11933, 2022.
- [27] C. Zheng, X. Yan, H. Zhang, B. Wang, S. Cheng, S. Cui, and Z. Li, "Beyond 3d siamese tracking: A motion-centric paradigm for 3d single object tracking in point clouds," in *Proceedings of the IEEE/CVF Conference on Computer Vision and Pattern Recognition*, pp. 8111–8120, 2022.
- [28] J. Long, E. Shelhamer, and T. Darrell, "Fully convolutional networks for semantic segmentation," in *Proceedings of the IEEE conference on computer vision and pattern recognition*, pp. 3431–3440, 2015.
- [29] C. R. Qi, L. Yi, H. Su, and L. J. Guibas, "Pointnet++: Deep hierarchical feature learning on point sets in a metric space," in *Advances in Neural Information Processing Systems*, vol. 30, Curran Associates, Inc., 2017.
- [30] Y. Yan, Y. Mao, and B. Li, "Second: Sparsely embedded convolutional detection," in *Sensors*, vol. 18, 2018.
- [31] X. Zhu, W. Su, L. Lu, B. Li, X. Wang, and J. Dai, "Deformable detr: Deformable transformers for end-to-end object detection," 2021.
- [32] X. Bai, Z. Hu, X. Zhu, Q. Huang, Y. Chen, H. Fu, and C.-L. Tai, "Transfusion: Robust lidar-camera fusion for 3d object detection with transformers," in *Proceedings of the IEEE/CVF Conference on Computer Vision and Pattern Recognition*, pp. 1090–1099, 2022.
- [33] B. Yan, X. Zhang, D. Wang, H. Lu, and X. Yang, "Alpha-refine: Boosting tracking performance by precise bounding box estimation," in *Proceedings of the IEEE/CVF Conference on Computer Vision and Pattern Recognition*, pp. 5289–5298, 2021.
- [34] T. Yin, X. Zhou, and P. Krahenbuhl, "Center-based 3d object detection and tracking," in *Proceedings of the IEEE/CVF conference on computer vision and pattern recognition*, pp. 11784–11793, 2021.
- [35] T.-Y. Lin, P. Goyal, R. Girshick, K. He, and P. Dollár, "Focal loss for dense object detection," in *Proceedings of the IEEE international conference on computer vision*, pp. 2980–2988, 2017.
- [36] A. Geiger, P. Lenz, and R. Urtasun, "Are we ready for autonomous driving? the kitti vision benchmark suite," in *IEEE Conference on Computer Vision and Pattern Recognition*, pp. 3354–3361, 2012.
- [37] H. Caesar, V. Bankiti, A. H. Lang, S. Vora, V. E. Liong, Q. Xu, A. Krishnan, Y. Pan, G. Baldan, and O. Beijbom, "nusscenes: A multimodal dataset for autonomous driving," in *IEEE/CVF Conference on Computer Vision and Pattern Recognition*, 2020.